CBPF-NF-013/03

Vacuum Energy Density of Conformally Coupled Fields in Rectangular Geometries

R.D.M. De Paola[b,*] *R.B. Rodrigues*[a,†], *and N.F. Svaiter*[a,‡]

[a]Centro Brasileiro de Pesquisas Fisicas-CBPF
Rua Dr. Xavier Sigaud 150, Rio de Janeiro, RJ, 22290-180, Brazil
[b]Instituto de Ciências - Escola Federal de Engenharia de Itajubá
Av. BPS 1303 Pinheirinho, 37500-903, Itajubá, MG - Brazil

Abstract

We calculate the vacuum energy density of the electromagnetic and conformally coupled scalar fields confined in the interior of a rectangular waveguide and of a rectangular cavity. We identify the physical measurable vacuum energy density by excluding local functions that once integrated do not depend on any global length parameters. Although this quantity is uniform for both fields between parallel plates we show that in the interior of the waveguide it is non-uniform for the conformally coupled scalar field and uniform for the electromagnetic field. In the interior of the rectangular cavity, it is non-uniform for the electromagnetic field. In the situations where the vacuum energy density is non-uniform, we provide a numerical analysis of the results, showing how their form depend on the boundary conditions and on the global length parameters.

Key-words: Quantum vacuum; Zero-point energy; Local effects; Renormalization.

*email: rpaola@efei.br
†email: robson@cbpf.br
‡email: nfuxsvai@cbpf.br

I. INTRODUCTION

It is well-known that boundary conditions imposed upon quantum fields may lead to divergent expectation values for local observables when they are evaluated on the boundaries. A simple example is a massless, minimally coupled scalar field $\varphi(t, \mathbf{x})$ which vanishes on the $z = 0$ plane. One finds that the renormalized expectation values of both φ^2 and of the energy density T_{00} diverge as $z \to 0$.

A less trivial example of the situation discussed above is the local version of Casimir original problem, performed by Brown and Maclay [1]. They obtained a finite (constant and diagonal) stress energy tensor due to the cancellation of the electric and magnetic sectors. This result can also be interpreted as due to the conditions of covariant conservation, null trace and symmetry considerations in the general form of the stress energy tensor between the plates [2] (a similar cancellation can be arranged for the scalar field by computing the improved stress energy tensor, which is traceless). Nevertheless, the boundedness (and uniformity) of the stress energy tensor of the electromagnetic field in this configuration does not represent its generic behavior. If the boundary is curved, however slightly, then the behavior of the stress energy tensor near the boundary is actually divergent. The electric and magnetic sectors in the Casimir problem each behave in this way, but the divergences cancel perfectly (see however [3]).

Though related to the infinities of field theory, this divergence is not of the usual type that is to be removed by renormalization. It is real in the sense that it originates in the unphysical nature of classical "perfect conductor" boundary conditions [2] [4]. In the case of material boundaries, such metal plates, infinite values of $\langle \mathbf{E}^2 \rangle$ or other observables are presumably avoided because such boundaries are not perfect reflectors at all frequencies. A metal plate is a good reflector of electromagnetic waves at frequencies below the plasma frequency, but becomes relatively transparent at higher frequencies (for a recent discussion see [5]).

A well-known example of the physical nature of boundary divergences is the wedge shaped region formed by two plane conducting boundaries intersecting at an angle α. We find [4] that $\langle T_{00}(x) \rangle$ diverges as r^{-4}, where r is the distance to the edge. In the limit $r \to \infty$ and $\alpha \to 0$ in such a way that $r\alpha = a$ remains constant, this configuration approaches two parallel plates separated by a distance a. This consistency would of course no be obtain if the unbounded term r^{-4} were to be removed by an *ad hoc* renormalization.

Consider a quantum field confined in the interior of a cavity with Dirichlet boundary conditions (although the correct picture of the Casimir effect is a classical boundary immersed in a quantum field, we will not lead with the contribution of external modes since this is a open problem for the rectangular boundaries considered is this paper; see for example ref. [6]). A fundamental problem is then how does the finite global Casimir effect result from the divergent local description. The traditional solution to this problem is to compare the system to a "reference vacuum" where the latter is understood to be the system obtained by displacing in an appropriate way all boundaries to spatial infinity [7] [8]. When local quantities are integrated over the cavity, this definition arranges the cancellation of the boundary divergences through the subtraction of a infinite quantity that do not depend on any global length parameters and then the global result is recovered. This infinity quantity is identified with the integral of the boundary divergent part over all space [9].

The global result can be obtained in another way, with a more clear physical interpretation, as the author showed in ref [9]. Explicit calculations for rectangular geometries demonstrated that the known global variable $\langle Q_m \rangle$ ($\langle\rangle$ means vacuum expectation value) of those systems can be obtained from the local variable $\langle Q(x) \rangle$ as follows :

$$\int_m \langle Q(x) \rangle_F = \langle Q_m \rangle + \int_{ext} \langle Q(x) \rangle_B \,, \tag{1.1}$$

where $\langle Q(x) \rangle_F$ and $\langle Q(x) \rangle_B$ means boundary finite and boundary divergent parts respectively. In the second integral, the subscript "*ext*" means that $\langle Q(x) \rangle_B$ is integrated outside the cavity far away where its diverges. To illustrate this, consider the scalar field between parallel plates separated by a distance a. The global energy can be obtained from the energy density (using the minimal coupled stress tensor) as :

$$\int_0^a \langle T_{00}(x) \rangle_F \, dx = E_c + \int_a^\infty (x)^{-2} \, dx + \int_{-\infty}^0 (x - a)^{-2} \, dx$$

where $E_c = \pi^2/1440a^4$ is the Casimir energy. Note that in the second member the integrals are convergent because the integrations are done away from the boundaries where the two integrands diverges.

Let us compare the two procedures. In the reference vacuum, the boundaries are infinitely far apart, so $\langle Q(x)\rangle_F = 0$. The physical measurable global variable $\langle Q_{phys}\rangle$ is defined by

$$\langle Q_{phys}\rangle = \int_m \langle Q(x)\rangle - \int_{all\ space} \langle Q(x)\rangle_B$$

Suppose that is possible to do the separation $\langle Q(x)\rangle = \langle Q(x)\rangle_F + \langle Q(x)\rangle_B$. Using (1.1) we have

$$\begin{aligned}\langle Q_{phys}\rangle &= \langle Q_m\rangle + \int_{ext} \langle Q(x)\rangle_B + \int_m \langle Q(x)\rangle_B - \int_{all\ space} \langle Q(x)\rangle_B \\ &= \langle Q_m\rangle\,.\end{aligned}$$

So the procedure of subtract a reference vacuum is equivalent to exclude the local functions that once integrated do not depend on any global length parameter. In this paper we define the physical measurable vacuum energy density using the latter procedure. Unlike the case of parallel planes geometry in which the conformally coupled scalar field and the electromagnetic field both gives a uniform vacuum energy density, we will show that these fields can give different answers (namely local functions uniform or not) in other rectangular geometries.

The organization of the paper is the following: In section II a brief review of the formalism is presented. In section III we calculate the boundary finite part of the vacuum energy density of a conformally coupled massless scalar field in a rectangular waveguide submitted to Dirichlet and Neumann boundary conditions on the walls. We then integrate the boundary finite part, separate the physical measurable vacuum energy density and show that it is non-uniform. A numerical analysis is presented to show how their form depend on the global length parameters. In section IV we use the Borgnis-Bromwich method to obtain the physical measurable energy density of the electromagnetic field in a rectangular waveguide and in a rectangular cavity. We show that this quantity is uniform in the waveguide configuration and non-uniform in the rectangular cavity. Conclusions are given in section V. In this paper we use $\hbar = c = 1$.

II. BASIC FORMALISM

A. Conformally coupled scalar field

The vacuum expectation value of the improved stress energy tensor of a real massless scalar field $\Theta_{\mu\nu}(x)$ can be written as

$$\langle\Theta_{\mu\nu}(x)\rangle = \lim_{y\to x}\left[\frac{1}{3}\left(\frac{\partial}{\partial x^\mu}\frac{\partial}{\partial y^\nu} + \frac{\partial}{\partial x^\nu}\frac{\partial}{\partial y^\mu}\right) - \frac{1}{6}\left(\frac{\partial}{\partial y^\mu}\frac{\partial}{\partial y^\nu} + \frac{\partial}{\partial x^\nu}\frac{\partial}{\partial x^\mu} + \eta_{\mu\nu}\frac{\partial}{\partial x^\alpha}\frac{\partial}{\partial y_\alpha}\right)\right]\langle\phi(x)\phi(y)\rangle\,, \tag{2.1}$$

Using the standard Fock space representation, the quantity $\langle\phi(x)\phi(y)\rangle$ in eq.(2.1), can be written as

$$\langle\phi(x)\phi(y)\rangle = \sum_n \frac{1}{2\omega_n}\exp(-i\,(x_0 - y_0)\,\omega_n)\phi_n(\mathbf{x})\phi_n^*(\mathbf{y})\ , \tag{2.2}$$

where $\mathbf{x} = (x_1, x_2, x_3)$ and $\{\phi_n(\mathbf{x})\}$ is a complete set of spatial modes satisfying $-\Delta\phi_n(\mathbf{x}) = \omega_n^2\phi_n(\mathbf{x})$. To simplify, let us limit the discussion to the energy density only. Applying the differential operator of eq.(2.1) in the expression given by eq.(2.2) and taking the limit $x \to y$ will define $\langle\Theta_{00}(\mathbf{x})\rangle$ (formally) as

$$\langle\Theta_{00}(\mathbf{x})\rangle = \frac{5}{12}\sum_n \omega_n\left|\phi_n\right|^2 + \frac{1}{12}\sum_n \frac{1}{\omega_n}\left|\vec{\nabla}\phi_n\right|^2 \tag{2.3}$$

The mode sums given by eq.(2.3) diverges and needs regularization and renormalization procedure. We can regularize these sums writing them in terms of the bilocal zeta function (and its spatial derivatives)

$$\langle \Theta_{00}(\mathbf{x}) \rangle = \frac{1}{12} \lim_{\mathbf{y}\to\mathbf{x}} \left[5\,\zeta(s=-\frac{1}{2} \mid \mathbf{x},\mathbf{y}) + \sum_{i=1}^{3} \frac{\partial}{\partial x^i}\frac{\partial}{\partial y^i}\zeta(s=\frac{1}{2} \mid \mathbf{x},\mathbf{y}) \right] \tag{2.4}$$

where :

$$\zeta\left(s \mid \mathbf{x},\mathbf{y}\right) = \mu^{2s} \sum_{n} \left(\omega_n^2\right)^{-s} \phi_n(\mathbf{x})\phi_n^*(\mathbf{y}), \tag{2.5}$$

(s complex) which in four space-time dimensions converges for $Re(s) > \frac{3}{2}$ (we introduce the parameter μ with dimensions of mass in order to have a dimensionless quantity raised to a complex power). As we have to calculate the bilocal zeta function in the region $Re(s) < \frac{3}{2}$ we have to define it through analytic continuation in s. It is related to the heat kernel by a Mellin transform

$$\zeta\left(s \mid \mathbf{x},\mathbf{y}\right) = \frac{\mu^{2s}}{\Gamma(s)} \int_0^\infty dt\, t^{s-1} K\left(t \mid \mathbf{x},\mathbf{y}\right), \qquad \mathrm{Re}\, s > \frac{3}{2} \tag{2.6}$$

where

$$K\left(t \mid \mathbf{x},\mathbf{y}\right) = \sum_{n} e^{-t\omega_n^2} \phi_n(\mathbf{x})\phi_n^*(\mathbf{y}), \qquad t > 0. \tag{2.7}$$

Initially holding $\mathrm{Re}\, s > \frac{3}{2}$ we can perform the Mellin transform of $K\left(t \mid \mathbf{x},\mathbf{y}\right)$ and then continued the result to $\mathrm{Re}\, s < \frac{3}{2}$. Once this is do it we can identify the free space bilocal zeta function (which has a ultraviolet divergence in the coincidence limit) and all boundary divergences. The remaining terms will form convergent mode sums. For sake of simplicity we choose $\mu = 1$ in the following because no final result in this work will depend on it.

B. Electromagnetic field

The stress energy tensor associated with the electromagnetic field can be calculated from the scalar problem using the Bromwich-Borgnis method [13], which reduces the problem to two scalar boundary value problems through the Hertz vectors. These quantities are connected with the electromagnetic potential in such a way that the Lorentz condition is satisfied identically. For given Hertzian vectors $\mathbf{\Pi}_e$ and $\mathbf{\Pi}_b$ the electric and magnetic fields are constructed by

$$\mathbf{E} = \nabla \times \nabla \times \mathbf{\Pi}_e + \frac{\partial\, \nabla \times \mathbf{\Pi}_b}{\partial\, t} \tag{2.8}$$

$$\mathbf{B} = \nabla \times \nabla \times \mathbf{\Pi}_b - \frac{\partial\, \nabla \times \mathbf{\Pi}_e}{\partial\, t} \tag{2.9}$$

We adopt the convention that the electric ($\mathbf{E}$) and magnetic ($\mathbf{H}$) fields are expressed in terms of the Hertz vectors having only one nonzero component

$$\mathbf{\Pi}_e = (0,\, 0,\, \phi), \quad \mathbf{\Pi}_b = (0,\, 0,\, \psi), \tag{2.10}$$

where ϕ and ψ are scalar fields that can be quantized as usual. Using the two preceding equations, the electric ($\mathbf{E}$) and magnetic ($\mathbf{B}$) fields are given by

$$\mathbf{E} = \left(\partial_0\partial_2\psi + \partial_1\partial_3\phi, -\partial_0\partial_1\psi + \partial_2\partial_3\phi, -\nabla_\perp^2\phi\right) \tag{2.11}$$

$$\mathbf{B} = \left(-\partial_0\partial_2\phi + \partial_1\partial_3\psi, \partial_0\partial_1\phi + \partial_2\partial_3\psi, -\nabla_\perp^2\psi\right) \tag{2.12}$$

where $\partial_\mu = \partial/\partial x^\mu$ and $\nabla_\perp^2 = \partial_1\partial_1 + \partial_2\partial_2$. The normalization constants for the electric and magnetic fields may be obtained demanding that

$$\int_{cavity} d^3x \frac{1}{2}\left(\mathbf{E}_{n_1,n_2,n_3}\mathbf{E}^*_{m_1,m_2,m_3} + \mathbf{B}_{n_1,n_2,n_3}\mathbf{B}^*_{m_1,m_2,m_3}\right) = \frac{1}{2}\omega\, \delta_{n_1m_1,n_2m_2,n_3m_3}$$

This condition is satisfied if the normalization constants are given by $|N_{n_1,n_2,n_3}|^2 = \nabla_\perp^{-2}$.

The vacuum stress energy tensor associated with the electromagnetic field

$$\langle T_{\alpha\beta}(\mathbf{x})\rangle = \lim_{\mathbf{y}\to\mathbf{x}} \left\langle F_{\alpha\mu}(\mathbf{x})F^{\mu}_{\beta}(\mathbf{y}) - \frac{1}{2}\eta_{\alpha\beta}F_{\mu\nu}(\mathbf{x})F^{\mu\nu}(\mathbf{y}) \right\rangle, \tag{2.13}$$

can be calculated using ϕ and ψ through the eqs.(2.11) and (2.12) by evaluating the appropriate electromagnetic field correlations. Again we will limit ourselves to the energy density only.:

$$\langle T_{00}(\mathbf{x})\rangle = \lim_{\mathbf{y}\to\mathbf{x}} \frac{1}{2}\left(\langle \mathbf{E}(\mathbf{x})\mathbf{E}(\mathbf{y})\rangle + \langle \mathbf{B}(\mathbf{x})\mathbf{B}(\mathbf{y})\rangle\right) \tag{2.14}$$

The electromagnetic boundary conditions $\mathbf{E}_\parallel = 0$ and $\mathbf{B}_\perp = 0$ on the walls will correspond to an appropriate combination of Dirichlet and Neumman boundary conditions for the scalar fields ϕ and ψ.

III. CONFORMALLY COUPLED SCALAR FIELD

A. Rectangular Waveguide

Let the waveguide be oriented along the x_3 axis, with Dirichlet (D) or Neumann (N) boundary conditions at $x_1 = 0$ and $x_1 = a$ and also $x_2 = 0$ and $x_2 = b$. For Dirichlet b.c., the spatial modes are given by:

$$\phi_{m_1,m_2}(\mathbf{x}) = \left(\frac{4}{ab}\right)^{\frac{1}{2}} \sin\frac{m_1\pi x_1}{a}\sin\frac{m_2\pi x_2}{b}\frac{1}{\sqrt{2\pi}}e^{ik_3x_3}, \tag{3.1}$$

with $m_{1,2} = 1, 2, 3, ...$; $-\infty < k_3 < \infty$ and $\omega_n^2 = \left(\left(\frac{m_1\pi}{a}\right)^2 + \left(\frac{m_2\pi}{b}\right)^2 + k_3^2\right)$, where n denotes the collective indices (m_1, m_2, k_3).

With Neumann b.c., the spatial modes are given by:

$$\phi_{m_1,m_2}(\mathbf{x}) = \left(\frac{4}{ab}\right)^{\frac{1}{2}} \cos\frac{m_1\pi x_1}{a}\cos\frac{m_2\pi x_2}{b}\frac{1}{\sqrt{2\pi}}e^{ik_3x_3}, \tag{3.2}$$

with $m_{1,2} = 0, 1, 2, 3, ...$ and $-\infty < k_3 < \infty$. Substituting eq.(3.1) in eq.(2.7), integrating the free space-time part using eq.(A1) and ressuming the resulting expression using eq.(A2) we have :

$$\begin{aligned} K(t \mid \mathbf{x},\mathbf{y}) &= (4\pi t)^{-\frac{3}{2}}\exp\left[-\frac{(x_3-y_3)^2}{4t}\right] \\ &\times \sum_{n_1=-\infty}^{\infty}\left\{\exp\left[\frac{-[2n_1a+(x_1-y_1)]^2}{4t}\right] \mp \exp\left[\frac{-[2n_1a+(x_1+y_1)]^2}{4t}\right]\right\} \\ &\times \sum_{n_2=-\infty}^{\infty}\left\{\exp\left[\frac{-[2n_2b+(x_2-y_2)]^2}{4t}\right] \mp \exp\left[\frac{-[2n_2b+(x_2+y_2)]^2}{4t}\right]\right\}. \end{aligned} \tag{3.3}$$

where the upper (lower) sign corresponds to Dirichlet (Neumann) boundary conditions. Performing the Mellin transform using eq.(A3) we have

$$\zeta(s \mid \mathbf{x},\mathbf{y}) = \frac{\Gamma(\frac{3}{2}-s)}{(4\pi)^{\frac{3}{2}}\Gamma(s)}\sum_{n_1,n_2=-\infty}^{\infty}\left(Z^{--} \mp Z^{-+} \mp Z^{+-} + Z^{++}\right), \tag{3.4}$$

where $Z^{\pm\pm} = Z^{\pm\pm}(n_1, n_2, \mathbf{x}, \mathbf{y})$ are given by

$$Z^{\pm\pm} = \left[\left(n_1a + \frac{(x_1 \pm y_1)}{2}\right)^2 + \left(n_2b + \frac{(x_2 \pm y_2)}{2}\right)^2 + \left(\frac{x_3-y_3}{2}\right)^2\right]^{s-\frac{3}{2}}. \tag{3.5}$$

Let us identify the ultraviolet and boundary divergences that will appear in the local zeta function $\zeta(s \mid \mathbf{x},\mathbf{x})$. The term $Z^{--}(0,0,\mathbf{x},\mathbf{y})$ is the free space-time contribution, then containing a ultraviolet divergence in the limit $\mathbf{y}\to\mathbf{x}$ and will be discarded. The terms $Z^{-+}(0,0,\mathbf{x},\mathbf{x})$, $Z^{-+}(0,-1,\mathbf{x},\mathbf{x})$, $Z^{+-}(0,0,\mathbf{x},\mathbf{x})$ and $Z^{+-}(-1,0,\mathbf{x},\mathbf{x})$ are identified with the divergent wall boundary terms and the terms $Z^{++}(0,0,\mathbf{x},\mathbf{x})$, $Z^{++}(0,-1,\mathbf{x},\mathbf{x})$, $Z^{++}(-1,0,\mathbf{x},\mathbf{x})$ and $Z^{++}(-1,-1,\mathbf{x},\mathbf{x})$ are identified with the divergent edge boundary terms. The appearance or not of these divergences in the stress energy tensor will depend on his specific form.

The energy density (2.4) can now be evaluated using the analytic continued bilocal zeta function (3.4) as

$$\langle\Theta_{00}(\mathbf{x})\rangle = \langle\Theta_{00}(\mathbf{x})\rangle_B + \langle\Theta_{00}(\mathbf{x})\rangle_F\,, \tag{3.6}$$

where B and F mean the boundary divergent and boundary finite part respectively. In explicit form:

$$\begin{aligned}\langle\Theta_{00}(\mathbf{x})\rangle_B &= -\frac{1}{96\pi^2}\{\Big[(x_1)^2+(x_2)^2\Big]^{-2}+\Big[(a-x_1)^2+(b-x_2)^2\Big]^{-2}+\\ &\quad+\Big[(x_1)^2+(b-x_2)^2\Big]^{-2}+\Big[(a-x_1)^2+(x_2)^2\Big]^{-2}\}\end{aligned} \tag{3.7}$$

$$\begin{aligned}\langle\Theta_{00}(\mathbf{x})\rangle_F &= -\frac{1}{32\pi^2}\sum_{(n_1,n_2)\neq(0,0)}\left[(n_1a)^2+(n_2b)^2\right]^{-2}+\\ &\pm\frac{1}{24\pi^2}\left(\sum(n_2b)^2\left[(n_1a+x_1)^2+(n_2b)^2\right]^{-3}+\sum(n_1a)^2\left[(n_1a)^2+(n_2b+x_2)^2\right]^{-3}\right)\\ &-\frac{1}{96\pi^2}\sum_{(n_1,n_2)\neq(0,0),(-1,-1),(0,-1),(-1,0)}\left[(n_1a+x_1)^2+(n_2b+x_2)^2\right]^{-2}.\end{aligned} \tag{3.8}$$

As expected we see that $\langle\Theta_{00}(\mathbf{x})\rangle$ has no wall divergences, but only edge ones.

Let us now integrate the boundary finite part of the vacuum energy density, $\langle\Theta_{00}(\mathbf{x})\rangle_F$, over the waveguide , $0\le x_1\le a, 0\le x_2\le b$, and separate the part that gives the total energy, i.e., the physical measurable part. The integral of the first term of eq.(3.8) gives:

$$-\frac{ab}{32\pi^2}Z_2(2|a,b), \tag{3.9}$$

where :

$$Z_2(2|a,b)=\sum_{(n_1,n_2)\neq(0,0)}\left[(n_1a)^2+(n_2b)^2\right]^{-2}.$$

The integration of the second (and third) term of eq.(3.8) can be done using the fact that

$$\int_0^a dx\sum_{n=-\infty}^{\infty}\left[(na+x)^2+B\right]^{-3}=\sum_{n=-\infty}^{\infty}\int_{na}^{(n+1)a}dt\left[t^2+B\right]^{-3}=2\int_0^{\infty}dt\left[t^2+B\right]^{-3}$$

where the last integral is given by eq.(A4). The result is :

$$-\frac{1}{24\pi^2}\int_0^a dx_1\int_0^b dx_2\sum\left[(n_1a+x_1)^2+(n_2b)^2\right]^{-3}(n_2b)^2=\frac{1}{32\pi a^2}\,\zeta(3), \tag{3.10}$$

$$-\frac{1}{24\pi^2}\int_0^a dx_1\int_0^b dx_2\sum\left[(n_2b+x_2)^2+(n_1a)^2\right]^{-3}(n_1a)^2=\frac{1}{32\pi b^2}\,\zeta(3), \tag{3.11}$$

where $\zeta(s)$ is the usual Riemann zeta function. Following the notation of [9], the integral of the fourth term of eq.(3.8) can be rewritten as:

$$-\frac{1}{96\pi^2}\int_0^a dx_1\int_0^b dx_2\;\zeta_F(2|x_1,x_2)=\frac{1}{96\pi^2}\int_{ext}\zeta_B(2|x_1,x_2)=$$
$$=\frac{1}{24\pi^2}\left[\int_a^\infty\int_b^\infty+\int_a^\infty\int_0^b+\int_0^a\int_b^\infty\right]dxdy\frac{1}{(x^2+y^2)^2}, \tag{3.12}$$

where

$$\zeta_F(2|x_1,x_2)=\sum_{(n_1,n_2)\neq(0,0)(0,-1)(-1,0)(-1,-1)}\left[(n_1a+x_1)^2+(n_2b+x_2)^2\right]^{-2} \tag{3.13}$$

and the right-hand side is each one of the divergent edge terms integrated over the appropriate quadrant *outside* the cavity, i.e., away of the points where they diverge, and thus eq.(3.12) is also finite but as we will see below, do not contribute to the total energy. Gathering all previous results we have that:

$$\int_{cavity}\langle\Theta_{00}(\mathbf{x})\rangle_F=E_C+\int_{ext}\langle\Theta_{00}(\mathbf{x})\rangle_B\,, \tag{3.14}$$

where

$$\int_{ext}\langle\Theta_{00}(\mathbf{x})\rangle_B=-\frac{1}{96\pi^2}\int_{ext}\zeta_B(2|x_1,x_2). \tag{3.15}$$

And

$$E_C=-\frac{ab}{32\pi^2}Z_2(2|a,b)+\frac{1}{32\pi}\zeta(3)\left(\frac{1}{a^2}+\frac{1}{b^2}\right), \tag{3.16}$$

is the total Casimir energy. We can add the same infinite term

$$\int_{cavity}\langle\Theta_{00}(\mathbf{x})\rangle_B$$

to both sides of the equation above, obtaining:

$$\int_{cavity}\langle\Theta_{00}(\mathbf{x})\rangle\;=\;E_C\;+\int_{all\;space}\langle\Theta_{00}(\mathbf{x})\rangle_B\,, \tag{3.17}$$

where the last integral above is an infinite constant independent of the global length parameters a, b. In global calculations one usually discards this infinite constant. The physical measurable energy density is then given by

$$\langle\Theta_{00}(\mathbf{x})\rangle_{phys}=-\frac{1}{32\pi^2}\sum_{(n_1,n_2)\neq(0,0)}\left[(n_1a)^2+(n_2b)^2\right]^{-2}+$$
$$\pm\frac{1}{24\pi^2}\sum\left[(n_2b)^2+(n_1a+x_1)^2\right]^{-3}(n_2b)^2+$$
$$\pm\frac{1}{24\pi^2}\sum\left[(n_1a)^2+(n_2b+x_2)^2\right]^{-3}(n_1a)^2. \tag{3.18}$$

Figure (1) show the form of $\langle\Theta_{00}(\mathbf{x})\rangle_{phys}$ in the interior of the square waveguide for Dirichlet b.c., assuming $a=b=1$. We see that this quantity is positive in all space points and produces a positive total energy. We observe that $\langle\Theta_{00}(\mathbf{x})\rangle_{phys}$ is greater near the edges. This result can be interpreted as though the edges mimic the curvature properties [10] once curved surfaces alter the local density of modes in the region near the surface. In general, the change in the mode density from the free-field case that occurs very near the surface varies as the inverse radius of the curvature [11]. Figure (2) show $\langle\Theta_{00}(\mathbf{x})\rangle_{phys}$ in the case $b=2a$. In this case the contribution of the negative part of the vacuum energy density dominates and one obtains a negative total energy.

Figure (3) show the form of $\langle\Theta_{00}(\mathbf{x})\rangle_{phys}$ in the interior of the square waveguide for Neumann b.c.. As Neumann boundary enhances the field in its vicinity, as opposite to Dirichlet boundary that weakens it, figure (3) has the form of the figure (1) upside down. Figure (4) shows $\langle\Theta_{00}(\mathbf{x})\rangle_e$ for $b=2a$. We see that in the Neumann case, the sign of the total energy do not change with the relative sizes of the waveguide as is well-know from global calculations [12].

B. Rectangular Cavity

For posterior use in the electromagnetic case, let us calculate the bilocal zeta function in the interior of a rectangular cavity submitted to mixed boundary conditions. Let the rectangular cavity obey Dirichlet boundary conditions at $x_1 = 0, a$ and $x_2 = 0, b$ and Neumann boundary conditions at $x_3 = 0, c$ (DDN). The spatial modes are given by:

$$\phi_{m_1,m_2,m_3}(\mathbf{x}) = \left(\frac{8}{abc}\right)^{\frac{1}{2}} \sin\frac{m_1\pi x_1}{a} \sin\frac{m_2\pi x_2}{b} \cos\frac{m_3\pi x_3}{c}, \tag{3.19}$$

with $m_{1,2} = 1, 2, 3, ...$, $m_3 = 0, 1, 2, 3...$and

$$\omega_n^2 = \left(\left(\frac{m_1\pi}{a}\right)^2 + \left(\frac{m_2\pi}{b}\right)^2 + (\frac{m_3\pi}{c})^2\right),$$

With Neumann boundary conditions at $x_1 = 0, a$ and $x_2 = 0, b$ and Dirichlet boundary conditions at $x_3 = 0, c$ (NND), the modes are :

$$\phi_{m_1,m_2,m_3}(\mathbf{x}) = \left(\frac{8}{abc}\right)^{\frac{1}{2}} \cos\frac{m_1\pi x_1}{a} \cos\frac{m_2\pi x_2}{b} \sin\frac{m_3\pi x_3}{c}, \tag{3.20}$$

with $m_{1,2} = 0, 1, 2, 3, ...$, $m_3 = 1, 2...$

Following the same steps of the previous subsection we have :

$$\zeta(s \mid \mathbf{x}, \mathbf{y}) = \frac{\Gamma(\frac{3}{2} - s)}{(4\pi)^{\frac{3}{2}}\Gamma(s)} \sum_{n_1,n_2,n_3=-\infty}^{\infty} \left(Z^{---} \mp Z^{+--} \mp Z^{-+-} \pm Z^{--+} + Z^{++-} - Z^{+-+} - Z^{-++} \pm Z^{+++}\right), \tag{3.21}$$

where the upper (lower) sign corresponds to DDN (NND) boundary conditions and $Z^{\pm\pm\pm} = Z^{\pm\pm\pm}(n_1, n_2, n_3, \mathbf{x}, \mathbf{y})$, are given by

$$Z^{\pm\pm\pm} = \left[\left(n_1 a + \frac{(x_1 \pm y_1)}{2}\right)^2 + \left(n_2 b + \frac{(x_2 \pm y_2)}{2}\right)^2 + \left(n_3 c + \frac{(x_3 \pm y_3)}{2}\right)^2\right]^{s-3/2}$$

The free space-time contribution $Z^{---}(0, 0, 0, \mathbf{x}, \mathbf{y})$ contain a ultraviolet divergence in limit $\mathbf{y}\to\mathbf{x}$ (will be discarded). The boundary divergences are contained in the following terms :

$Z^{+--}(0, 0, 0, \mathbf{x}, \mathbf{x})$, $Z^{+--}(-1, 0, 0, \mathbf{x}, \mathbf{x})$, $Z^{-+-}(0, 0, 0, \mathbf{x}, \mathbf{x})$, $Z^{-+-}(0, -1, 0, \mathbf{x}, \mathbf{x})$, $Z^{--+}(0, 0, 0, \mathbf{x}, \mathbf{x})$ and $Z^{--+}(0, 0, -1, \mathbf{x}, \mathbf{x}) \Rightarrow$ divergent wall boundary terms.

$Z^{++-}(0, 0, 0, \mathbf{x}, \mathbf{x})$, $Z^{++-}(0, -1, 0, \mathbf{x}, \mathbf{x})$, $Z^{++-}(-1, 0, 0, \mathbf{x}, \mathbf{x})$, $Z^{++-}(-1, -1, 0, \mathbf{x}, \mathbf{x})$, $Z^{+-+}(0, 0, 0, \mathbf{x}, \mathbf{x})$, $Z^{+-+}(-1, 0, 0, \mathbf{x}, \mathbf{x})$, $Z^{+-+}(0, 0, -1, \mathbf{x}, \mathbf{x})$, $Z^{+-+}(-1, 0, -1, \mathbf{x}, \mathbf{x})$, $Z^{-++}(0, 0, 0, \mathbf{x}, \mathbf{x})$, $Z^{-++}(0, -1, 0, \mathbf{x}, \mathbf{x})$, $Z^{-++}(0, 0, -1, \mathbf{x}, \mathbf{x})$ and $Z^{-++}(0, -1, -1, \mathbf{x}, \mathbf{x}) \Rightarrow$ divergent edge boundary terms.

$Z^{+++}(0, 0, 0, \mathbf{x}, \mathbf{x})$, $Z^{+++}(-1, 0, 0, \mathbf{x}, \mathbf{x})$, $Z^{+++}(0, -1, 0, \mathbf{x}, \mathbf{x})$, $Z^{+++}(0, 0 - 1, \mathbf{x}, \mathbf{x})$, $Z^{+++}(-1, -1, 0, \mathbf{x}, \mathbf{x})$, $Z^{+++}(-1, 0, -1, \mathbf{x}, \mathbf{x})$, $Z^{+++}(0, -1, -1, \mathbf{x}, \mathbf{x})$ and $Z^{+++}(-1, -1, -1, \mathbf{x}, \mathbf{x}) \Rightarrow$divergent corner boundary terms.

IV. ELECTROMAGNETIC FIELD

A. Rectangular Cavity

In the case of a rectangular cavity, it turns out that the boundary conditions of the electromagnetic field at the inner surface of the cavity are fulfilled if ϕ satisfies Dirichlet boundary conditions at the walls which are parallel to the e_3 direction and Neumman boundary conditions at the walls perpendicular to e_3 and exactly the other way

around for the potential ψ. Thus the bilocal zeta functions defined by eq. (3.21), $\zeta(s\,|\mathbf{x},\mathbf{y})_{DDN}$ and $\zeta(s\,|\mathbf{x},\mathbf{y})_{NND}$ are the bilocal zeta functions for the potentials ϕ and ψ respectively.

For brevity let us evaluate only the boundary finite part of the energy density (the other components can be calculated exactly in the same way). It is easy to show that by evaluating the electromagnetic field correlations present in eq.(2.14) using eqs.(2.11) and (2.12), the resulting expression will depend only on derivatives of $\langle\phi(x)\phi(y)\rangle + \langle\psi(x)\psi(y)\rangle$. After a long but straightforward calculation we get

$$\begin{aligned}
\langle T_{00}(\mathbf{x})\rangle_F = &-\frac{1}{16\pi^2}\sum_{(n_1,n_2,n_3)\neq(0,0,0)}\left[(n_1a)^2+(n_2b)^2+(n_3c)^2\right]^{-2}+\\
&-\frac{1}{16\pi^2}\sum_{(n_1,n_2,n_3)\neq(0,0,0),(0,-1,-1),(0,0,-1),(0,-1,0)}\left[(n_1a)^2+(n_2b+x_2)^2+(n_3c+x_3)^2\right]^{-2}+\\
&+\frac{1}{4\pi^2}\sum_{(n_1,n_2,n_3)\neq(0,0,0),(0,-1,-1),(0,0,-1),(0,-1,0)}\left[(n_1a)^2+(n_2b+x_2)^2+(n_3c+x_3)^2\right]^{-3}(n_1a)^2+\\
&-\frac{1}{16\pi^2}\sum_{(n_1,n_2,n_3)\neq(0,0,0),(-1,0,-1),(0,0,-1),(-1,0,0)}\left[(n_1a+x_1)^2+(n_2b)^2+(n_3c+x_3)^2\right]^{-2}+\\
&+\frac{1}{4\pi^2}\sum_{(n_1,n_2,n_3)\neq(0,0,0),(-1,0,-1),(0,0,-1),(-1,0,0)}\left[(n_1a+x_1)^2+(n_2b)^2+(n_3c+x_3)^2\right]^{-3}(n_2b)^2+\\
&-\frac{1}{16\pi^2}\sum_{(n_1,n_2,n_3)\neq(0,0,0),(-1,-1,0),(0,-1,0),(-1,0,0)}\left[(n_1a+x_1)^2+(n_2b+x_2)^2+(n_3c)^2\right]^{-2}+\\
&+\frac{1}{4\pi^2}\sum_{(n_1,n_2,n_3)\neq(0,0,0),(-1,-1,0),(0,-1,0),(-1,0,0)}\left[(n_1a+x_1)^2+(n_2b+x_2)^2+(n_3c)^2\right]^{-3}(n_3c)^2, \qquad (4.1)
\end{aligned}$$

where in the first sum we excluded the free space-time divergence and in other sums we excluded the edges divergences (the wall and corner divergences have been cancelled when we combined the Hertz potentials).

Let us now integrate the boundary finite part of the vacuum energy density, $\langle T_{00}(\mathbf{x})\rangle_F$, over the cavity , $0\le x_1\le a, 0\le x_2\le b, 0\le x_3\le c$, and separate the part that gives the total energy. The integral of the first term of eq.(4.1) gives:

$$-\frac{abc}{16\pi^2}Z_3(2|a,b,c), \qquad (4.2)$$

where

$$Z_3(2|a,b,c)=\sum_{(n_1,n_2)\neq(0,0,0)}\left[(n_1a)^2+(n_2b)^2+(n_3c)^2\right]^{-2}. \qquad (4.3)$$

Following again the notation of [9] and using (A4), the integral of the second term gives :

$$\begin{aligned}
&-\frac{1}{8\pi^2}\int_0^a dx_1\int_0^b dx_2\int_0^c dx_3\left\{\zeta_F(2|x_2,x_3)+\sum_{n_{2,3}=-\infty}^{\infty}\sum_{n_1\neq0}\left[(n_1a)^2+(n_2b+x_2)^2+(n_3c+x_3)^2\right]^{-2}\right\}\\
&=-\frac{a}{8\pi^2}\int_{ext}\zeta_B(2|x_2,x_3)-\frac{\pi}{48a}, \qquad (4.4)
\end{aligned}$$

where the functions $\zeta_F(2|x_2,x_3)$ and $\zeta_B(2|x_2,x_3)$ are defined by eqs. (3.13) and (3.12). The integral of the third term gives :

$$\frac{1}{4\pi^2}\int_0^a dx_1\int_0^b dx_2\int_0^c dx_3\sum_{n_{2,3}=-\infty}^{\infty}\sum_{n_1\neq0}\left[(n_1a)^2+(n_2b+x_2)^2+(n_3c+x_3)^2\right]^{-3}(n_1a)^2=\frac{\pi}{24a} \qquad (4.5)$$

The other terms can be integrated in a similar way. Gathering all previous results we have

$$\int\int_{cavity} \langle T_{00}(\mathbf{x})\rangle_F = E_C + \int_{ext} \langle T_{00}(\mathbf{x})\rangle_B \,, \tag{4.6}$$

where

$$E_C = -\frac{abc}{16\pi^2} Z_3(2|a,b,c) + \frac{\pi}{48}\left(\frac{1}{a}+\frac{1}{b}+\frac{1}{c}\right) \tag{4.7}$$

is the total Casimir energy, in agreement with [8] and

$$\int_{ext} \langle T_{00}(\mathbf{x})\rangle_B = -\frac{1}{8\pi^2}\left\{a\int_{ext}\zeta_B(2|x_2,x_3) + b\int_{ext}\zeta_B(2|x_1,x_3) + c\int_{ext}\zeta_B(2|x_1,x_2)\right\}. \tag{4.8}$$

Finally, the physical measurable vacuum energy density is :

$$\begin{aligned}
\langle T_{00}(\mathbf{x})\rangle_{phys} =& -\frac{1}{16\pi^2}\sum_{(n_1,n_2,n_3)\neq(0,0,0)}\left[(n_1a)^2+(n_2b)^2+(n_3c)^2\right]^{-2} + \\
&-\frac{1}{16\pi^2}\sum_{n_{2,3}=-\infty}^{\infty}\sum_{n_1\neq 0}\left[(n_1a)^2+(n_2b+x_2)^2+(n_3c+x_3)^2\right]^{-2} + \\
&+\frac{1}{4\pi^2}\sum_{n_{2,3}=-\infty}^{\infty}\sum_{n_1\neq 0}\left[(n_1a)^2+(n_2b+x_2)^2+(n_3c+x_3)^2\right]^{-3}(n_1a)^2 + \\
&-\frac{1}{16\pi^2}\sum_{n_{1,3}=-\infty}^{\infty}\sum_{n_2\neq 0}\left[(n_1a+x_1)^2+(n_2b)^2+(n_3c+x_3)^2\right]^{-2} + \\
&+\frac{1}{4\pi^2}\sum_{n_{1,3}=-\infty}^{\infty}\sum_{n_2\neq 0}\left[(n_1a+x_1)^2+(n_2b)^2+(n_3c+x_3)^2\right]^{-3}(n_2b)^2 + \\
&-\frac{1}{16\pi^2}\sum_{n_{1,2}=-\infty}^{\infty}\sum_{n_3\neq 0}\left[(n_1a+x_1)^2+(n_2b+x_2)^2+(n_3c)^2\right]^{-2} + \\
&+\frac{1}{4\pi^2}\sum_{n_{1,2}=-\infty}^{\infty}\sum_{n_3\neq 0}\left[(n_1a+x_1)^2+(n_2b+x_2)^2+(n_3c)^2\right]^{-3}(n_3c)^2.
\end{aligned} \tag{4.9}$$

And we see that this is a non-uniform function. Its form is show in figure (5) for $a=b=c=1$ at the $z=1/2$, $z=1/4$ and $z=1/16$ planes respectively. We see that the vacuum energy density grows as we approach the corners (as expected).

B. Rectangular Waveguide

Letting the waveguide be oriented along the x_3 axis, it follows that ϕ and ψ must satisfy Dirichlet and Neumann boundary conditions, respectively. Therefore, the bilocal zeta functions associated with the Hertz potentials ϕ and ψ are given by eq. (3.4). Following the same steps of the previous section we have for the boundary finite part of the vacuum energy density

$$\begin{aligned}
\langle T_{00}(\mathbf{x})\rangle_F =& -\frac{1}{16\pi^2}\sum_{(n_1,n_2)\neq(0,0)}\left[(n_1a)^2+(n_2b)^2\right]^{-2} + \\
&-\frac{1}{16\pi^2}\sum_{(n_1,n_2)\neq(0,0),(-1,-1),(0,-1),(-1,0)}\left[(n_1a+x_1)^2+(n_2b+x_2)^2\right]^{-2}
\end{aligned} \tag{4.10}$$

where we excluded the free space-time divergence in the first sum and the edges divergences in the second sum (the wall divergences was cancelled when we combined the Hertz potentials). Like in the case of the conformally coupled scalar field the second term do not contribute to the global energy, therefore the physical measurable energy

density is only the first term, which is uniform. So we have showed that in the waveguide configuration, besides the fact that the wall divergences cancelled for conformally coupled scalar field and for the electromagnetic field, the physical measurable energy density is non-uniform in the first case and uniform in the second.

V. CONCLUSIONS

In this paper we obtained the physical measurable vacuum energy density of a massless scalar field in a rectangular waveguide and of a electromagnetic field in a rectangular waveguide and in a rectangular cavity. As we showed, in the waveguide configuration this quantity is non-uniform for the conformally coupled scalar field and uniform for the electromagnetic field. The numerical analysis illustrated how their form depend on the boundary conditions and on the sizes of the waveguide. This result can be though as an unexpected since as we mentioned in the introduction, in the Casimir original problem the uniformity of the vacuum energy density is usually associated with the fact that the stress energy tensor of the electromagnetic field is traceless. Nevertheless, in a rectangular cavity, we showed that the physical measurable energy density is non-uniform for the electromagnetic field. The discrepancy between the results is probably attributed to the number of degrees of freedom of each one these fields.

Although the global Casimir effect is more related to experiments where we measure the force between macroscopic surfaces, we believe that the local Casimir description has physical relevance since the stress energy tensor is in principle an unambiguously identified quantity, by its effect on the gravitational field. In the context of the perfect conductor model, it is reasonable to associate the results obtained in this paper as the source of the gravitational field since as we mentioned we identify the physical measurable part of the stress energy tensor by discarding an infinity quantity that do not depend on any global parameter.

In order to remove the boundary divergences, two possible ways are to take into account the real properties of the material, i.e., imperfect conductivity at high frequencies, or else make a quantum mechanical treatment of the boundary conditions, as was done by Ford and Svaiter [14]. It should be interesting to repeat the present investigation about the uniformity of the vacuum energy density using these possibilities.

VI. ACKNOWLEDGMENTS

This paper is supported by the Conselho Nacional de Desenvolvimento Cientifico e Tecnológico do Brasil (CNPq), and by Fundação de Amparo à Pesquisa do Estado de Minas Gerais (FAPEMIG).

APPENDIX A: FORMULAE

$$\frac{1}{2\pi}\int dk_3\, e^{-t(k_3)^2} e^{ik_3(x_3-y_3)} = (4\pi t)^{-\frac{1}{2}} \exp\left[-\frac{(x_3-y_3)^2}{4t}\right], \tag{A1}$$

Jacobi θ-function identity

$$\sum_{m=1}^{\infty} \exp(-m^2 x)\cos(m2\pi h) = -\frac{1}{2} + \sqrt{\frac{\pi}{4x}} \sum_{n=-\infty}^{\infty} \exp\left[-(n+h)^2\frac{\pi^2}{x}\right] \tag{A2}$$

$$\int_0^{\infty} dt\, t^{s-\frac{5}{2}} \exp(-\frac{A}{t}) = A^{s-\frac{3}{2}}\Gamma(\frac{3}{2}-s), \qquad \mathrm{Re}\, s > \frac{3}{2}. \tag{A3}$$

$$2\int_0^{\infty} dt \left[\, t^2 + B\right]^{s-2} = B^{s-\frac{3}{2}} \frac{\sqrt{\pi}\Gamma(\frac{3}{2}-s)}{\Gamma(2-s)}. \tag{A4}$$

[1] L.H. Brown and G.J. Maclay, Phys. Rev. **184**, 1272 (1976).

[2] B.S. DeWitt, Phys. Rep. **19**, 259 (1975).

[3] L.H. Ford and V. Sopova, Phys. Rev. **D66**, 045026, (2002).

[4] D. Deutsch and P. Candelas, Phys. Rev. **D20**, 3063 (1979).

[5] S. A. Fulling, "Systematics of the Relationship between Vacuum Energy Calculations and Heat Kernel Coefficients", [arXiv:quant-ph/0302117].

[6] N.F. Svaiter and B.F. Svaiter, J.Phys. A **25**, 979-989 (1992).

[7] G. Plunien, B. Müller and W. Greiner, Phys. Rep. **134**, 87 (1986).

[8] W. Lukosz, Physica **56,** 109 (1971); Z.Phys. **262,** 327 (1973).

[9] A.A. Actor, Ann. Phys. **230**, 303 (1994); Fortschr. Phys. **43**, 141 (1995).

[10] A.A. Actor and I. Bender, Fortschr. Phys. **44**, 281 (1996).

[11] G.J. Maclay, Phys.Rev.**A61**, 052110 (2000).

[12] J.S. Dowker and G. Kennedy, J. Phys. **A11**, 895 (1978).

[13] E. Borgnis and C. H. Papas, Electromagnetic Waveguides and Resonators, *in* "Encyclopedia of Physics," v. XVI, pp. 285–422 (S. Flüge, Ed.), Springer Verlag, Berlin, 1958.

[14] L.H. Ford and N.F. Svaiter, Phys. Rev. **D58**, 065007-1, (1998).

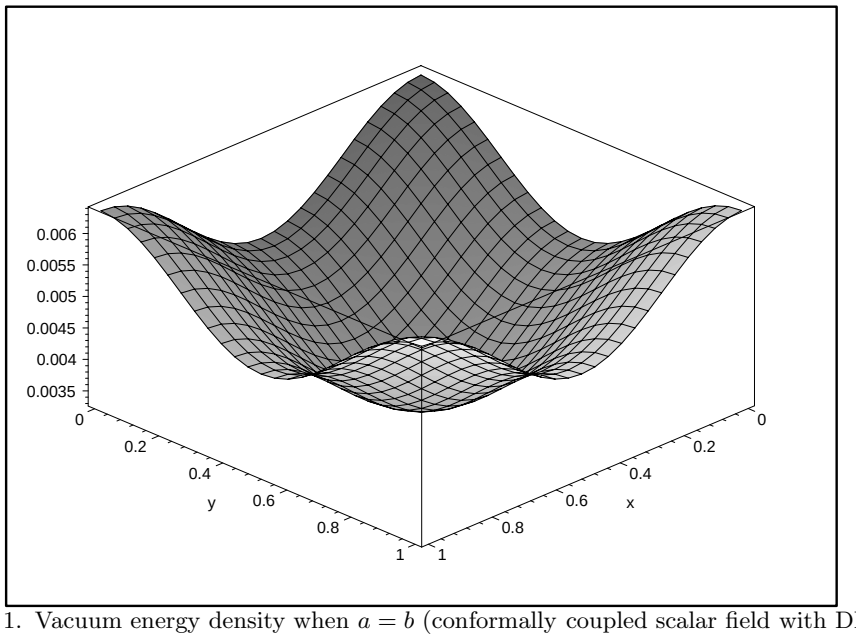

FIG. 1. Vacuum energy density when $a = b$ (conformally coupled scalar field with DBC).

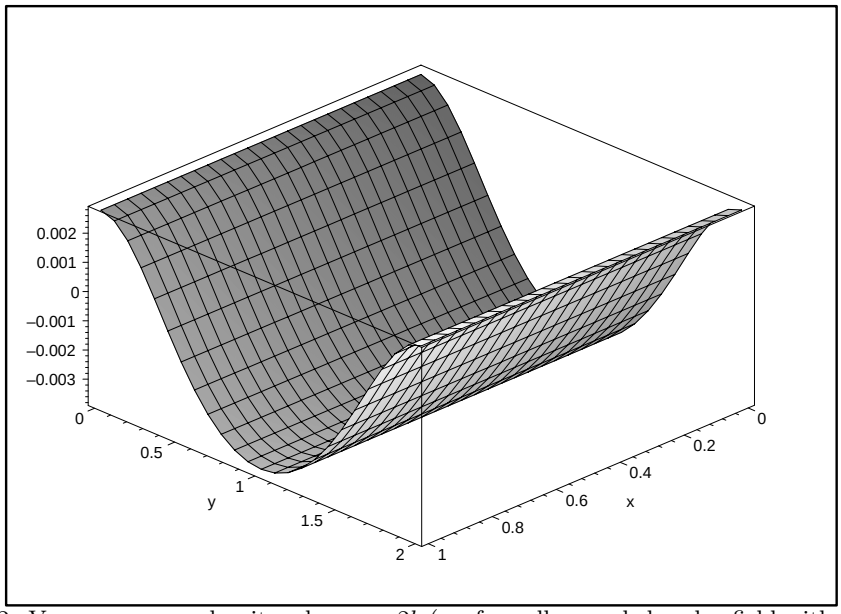

FIG. 2. Vacuum energy density when $a = 2b$ (conformally coupled scalar field with DBC).

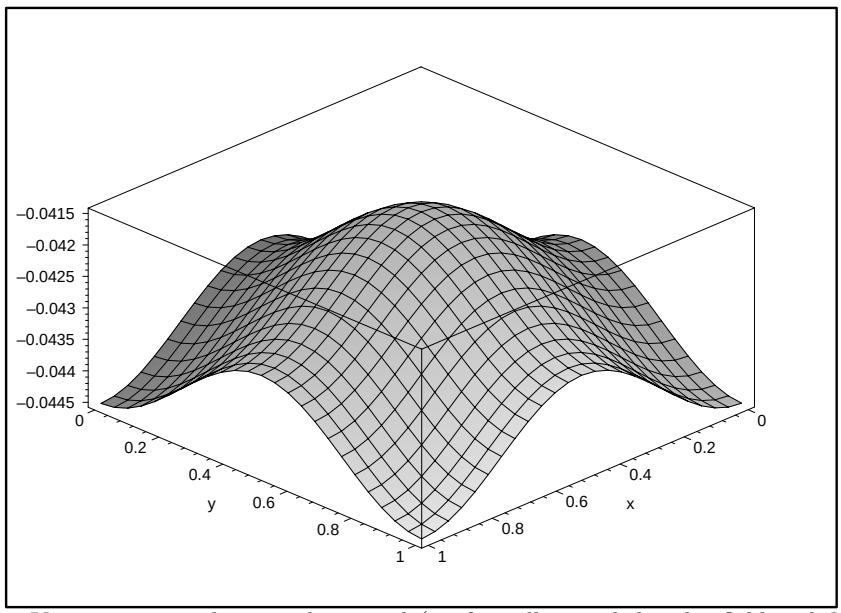

FIG. 3. Vacuum energy density when $a = b$ (conformally coupled scalar field with NBC) .

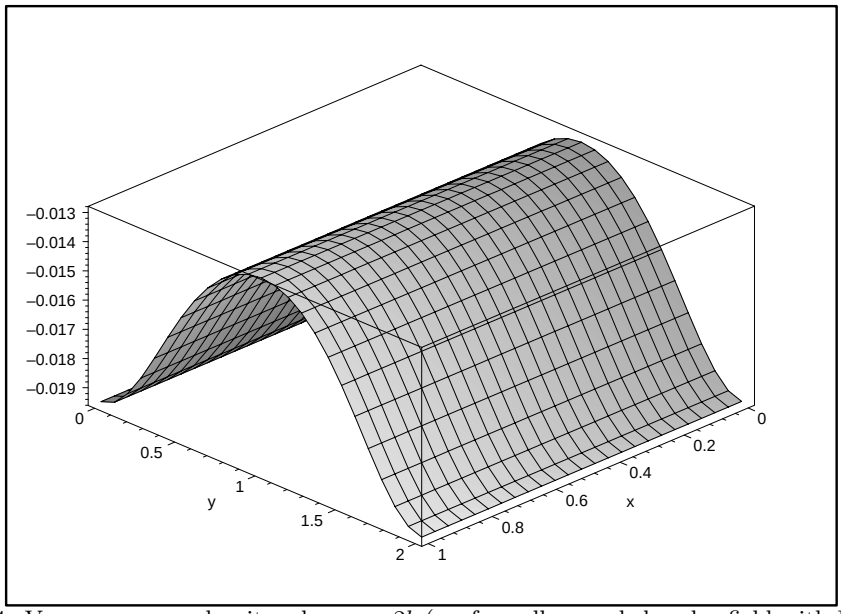

FIG. 4. Vacuum energy density when $a = 2b$ (conformally coupled scalar field with NBC) .

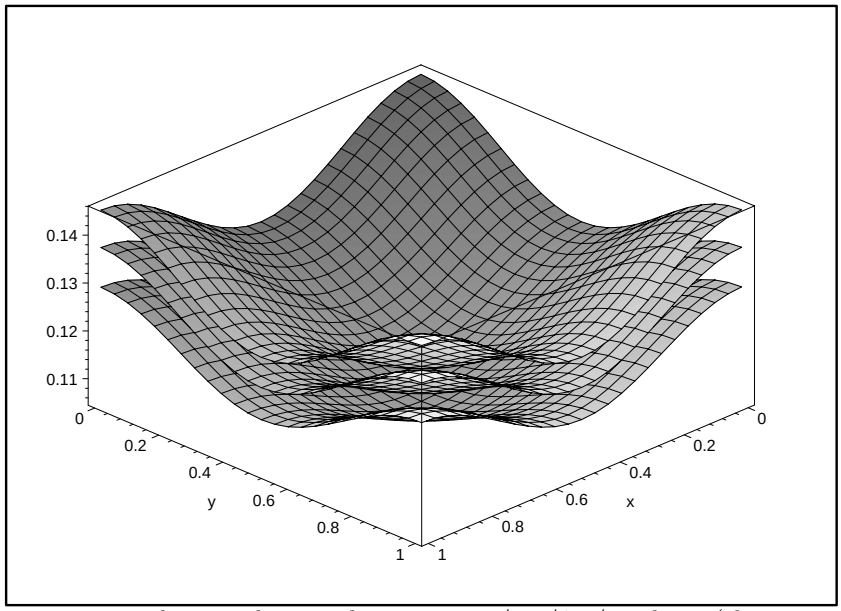

FIG. 5. Vacuum energy density when $a = b = c$ at $z = 1/2, 1/4, 1/16$ planes (electromagnetic field).